



Cite this: *Chem. Commun.*, 2024, **60**, 11770

Received 9th July 2024,
Accepted 16th September 2024

DOI: 10.1039/d4cc03430a

rsc.li/chemcomm

Guanidinium organosulfonate (GS) hydrogen-bonded host frameworks were used to trap α -halopropiophenones and α -halocyclooctanones to determine their molecular structure by single crystal X-ray diffraction. The majority of encapsulated guest molecules adopted conformations expected from computational analysis and stereochemical outcomes of Grignard reactions.

Guanidinium organosulfonate (GS) hydrogen-bonded frameworks have been deployed for a variety of applications,^{1,2} owing their utility to a persistent hydrogen-bonded network of charge-assisted hydrogen bonds between complementary guanidinium cations ($\text{G, C}(\text{NH}_2)_3^+$) and organosulfonate anions (S) (Fig. 1A).³ These frameworks readily form stoichiometric inclusion compounds with a wide range of guests.^{4,5} Puckering of the GS sheet and conformational flexibility of some organosulfonates allow the framework to “shrink wrap” around guests and achieve optimal packing density. Moreover, a given GS framework can adopt various architectures that adapt to the size and shape of guest molecules.

Our laboratories previously reported the encapsulation of 2-chloropropiophenone as a guest within a GS host framework. The conformation of this ketone guest corroborated the stereochemical outcome of the nucleophilic addition of allylmagnesium halide to 2-chloropropiophenone (Fig. 2A).⁶ Moreover, the conformation of the 2-chloropropiophenone guest closely resembled that predicted by the polar Felkin–Anh stereochemical model, in which the carbon–chlorine bond is oriented to maximize hyperconjugative interactions ($\sigma_{\text{C–Cl}} \rightarrow \pi_{\text{C–O}}^*$) with the carbon–oxygen bond (Fig. 2B). Nucleophilic attack on this conformational isomer occurred on the diastereoface opposite the chlorine atom (Fig. 2C),⁶ resulting in high diastereoselectivity for the 1,2-*anti* alcohol product. Encapsulation within the framework enables analysis of the substrate conformations associated with these reactions.

Department of Chemistry, New York University, New York City, New York, 10003, USA

† Electronic supplementary information (ESI) available. CCDC 2364251–2364258. For ESI and crystallographic data in CIF or other electronic format see DOI: <https://doi.org/10.1039/d4cc03430a>

Hydrogen-bonded frameworks for conformational analysis of reactive substrates†

Alexandra M. Dillon, Alexander G. Shtukenberg, Krystyna M. Demkiw, K. A. Woerpel * and Michael D. Ward *

A series of α -halopropiophenones were encapsulated in GS host frameworks. Three different GS hosts were employed to ascertain their influence (or absence thereof) on the preferred conformations of these guest molecules and whether the conformations corroborate the stereochemical outcomes of their Grignard reactions. This approach was extended to other α -halogenated ketones.

α -Halopropiophenones. Three α -halopropiophenones, which exist as liquids at room temperature, were encapsulated separately in guanidinium cyclohexanemonosulfonate (GCHMS), guanidinium 4,4'-biphenyldisulfonate (G_2BPDS), and guanidinium 1,5-naphthalenedisulfonate ($\text{G}_2\text{1,5-NDS}$) host frameworks by single-step crystallization in methanol and ethanol (Fig. 1B). These frameworks were selected because they exhibit varying degrees of freedom with respect to achieving dense packing, permitting exploration of the influence of the host on the

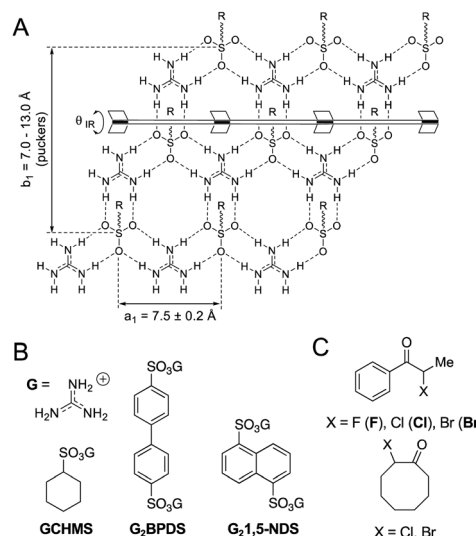


Fig. 1 (A) Hydrogen-bonded sheet formed by guanidinium and organosulfonate ions. The sheet consists of one-dimensional GS “ribbons” joined by hydrogen bonds along their edges, serving as “hinges” that permit puckering, denoted as the inter-ribbon angle (θ_{IR}). (B) and (C) Molecular structures of GS hosts and guest molecules.

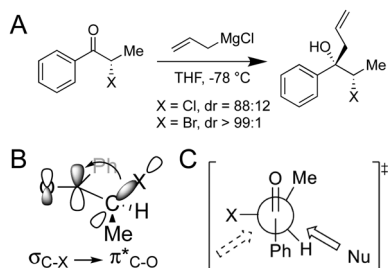


Fig. 2 (A) Reaction of 2-chloro- and 2-bromopropiophenone with allylmagnesium chloride. (B) Hyperconjugative interactions of $\sigma_{C-X} \rightarrow \pi_{C-O}^*$. (C) Newman projection showing the polar Felkin–Anh transition state in nucleophilic attack to α -halopropiophenones.

conformation of the guest. GCHMS inclusion compounds are not constrained by covalent connections between opposing GS sheets,⁷ unlike G₂BPDS and G₂1,5-NDS hosts. Rotation of the phenyl rings in G₂BPDS can facilitate packing of guest molecules between the GS sheets, but the rigid core of the naphthalene moiety in G₂1,5-NDS can frustrate dense packing.

Single crystal X-ray diffraction was used to characterize the structure of nine inclusion compounds derived from racemic mixtures of 2-fluoropropiophenone (**F**), 2-chloropropiophenone (**Cl**), and 2-bromopropiophenone (**Br**) (Fig. 1C) in GCHMS, G₂BPDS, and G₂1,5-NDS. The various architectures formed by these inclusion compounds can be described by the projection topologies of their organic residues from either side of the GS sheet (Fig. S1, ESI†).⁷ (GCHMS)₄ \supset **Cl** and (GCHMS)₄ \supset **Br** adopted the recently reported “tetrad II” architecture (Fig. 3).⁷ GCHMS \supset **F** formed the “s-CLIC” host architecture, but refinement of the guest was not possible owing to disorder of the guest along channels. G₂BPDS \supset **F** adopted a “bilayer” architecture, while G₂BPDS \supset **Br** and G₂BPDS \supset **Cl**⁶ formed a unique “bilayer” architecture with water molecules bridging adjacent bilayers. The G₂1,5-NDS inclusion compounds assembled in the simple brick architecture, although the hydrogen-bonding motif in the GS sheet of G₂1,5-NDS \supset **Br** departs slightly from the typical quasi-hexagonal motif, with one fewer hydrogen bond than the customary six (Fig. S3, ESI†).³ All crystallization experiments were performed with a racemic mixture of guests. G₂1,5-NDS \supset **Br** crystallized as a conglomerate in the enantiomeric *P*₂₁ space group. All other structures contain both enantiomers in equal amounts.

The conformations of the α -halopropiophenone guests in all the inclusion compounds can be classified, according to their O–C–C–X dihedral angles ($\phi_{O-C-C-X}$), as “anticlinal,” “gauche,” and “synperiplanar,” with $\phi_{O-C-C-X} = 135^\circ$ to -135° , $|45^\circ$ – $135^\circ|$, and -45° to 45° , respectively (Fig. 4 and Fig. S2, ESI†). The synperiplanar conformation of **F** was confirmed in G₂1,5-NDS. The gauche conformation of **Cl** was confirmed in G₂BPDS. The gauche conformation of **Br** was confirmed in all three host frameworks (Fig. 4). Conformation assignments of **Cl** in GCHMS and G₂1,5-NDS, and **F** in G₂BPDS were ambiguous due to positional disorder of the guests that made it difficult to localize the halogen atom during refinement and distinguish the halogen from the methyl group. The anticlinal conformation could be ruled out in each case, however.

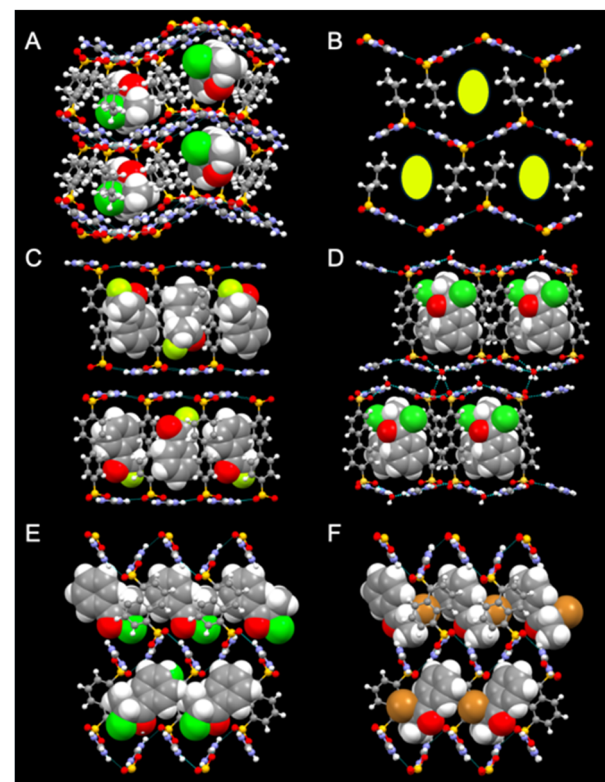


Fig. 3 (A) (GCHMS)₄ \supset **Cl**. (B) GCHMS \supset **F**. The lime-colored ovals represent disordered guests that could not be refined. (C) G₂BPDS \supset **Cl**. (D) G₂BPDS \supset **Cl**. (E) G₂1,5-NDS \supset **Cl**. (F) G₂1,5-NDS \supset **Br**. The GS frameworks are depicted as ball-and-stick and the guest molecules as space-filling.

The experimentally determined conformations can be understood by comparison to the calculated conformational preferences. Computational studies (at the M06-2X/6-311+G(d,p) level) have suggested a favored *gauche* conformation for **Br** and **Cl**, with a stronger preference in the case of **Br**.⁸ The *gauche* conformation maximizes $\sigma_{C-X} \rightarrow \pi_{C-O}^*$ hyperconjugation (Fig. 2B), which is particularly favored for **Br** over **Cl** because the carbon–bromine bond is the stronger electron donor.^{6,8} In contrast, the lowest energy conformer calculated for **F** was *anticlinal*, with $\phi_{O-C-C-X} = -149^\circ$, consistent with σ_{C-F} being a weaker electron donor relative to the other carbon–halogen bonding orbitals, as indicated by $\sigma_{C-X} \rightarrow \pi_{C-O}^*$ stabilization energies: σ_{C-F} (1.68 kcal mol⁻¹) $<$ σ_{C-Cl} (5.33 kcal mol⁻¹) $<$ σ_{C-Br} (7.65 kcal mol⁻¹).⁸ The *synperiplanar* conformation of **F** was favored in polar solvents, however (ca. 70% in methanol).⁸ This result suggests that the *synperiplanar* **F** conformer in G₂1,5NDS \supset **F** reflects the dominant conformer in methanol, the crystallization solvent. Despite the effectively identical number of electrons in the fluoro and methyl group, which can make it difficult to distinguish their positions, the refinement was sufficient to ascertain bond lengths and confirm the *synperiplanar* conformer in G₂1,5NDS \supset **F**, unlike G₂BPDS \supset **F**.

The crystal structures based on the G₂1,5NDS host reveal a competition between sustaining hydrogen bonds in the GS sheet and the conformational preference of the guest. The simple brick architecture in the G₂1,5NDS inclusion compounds affords channels perpendicular to the puckering axis

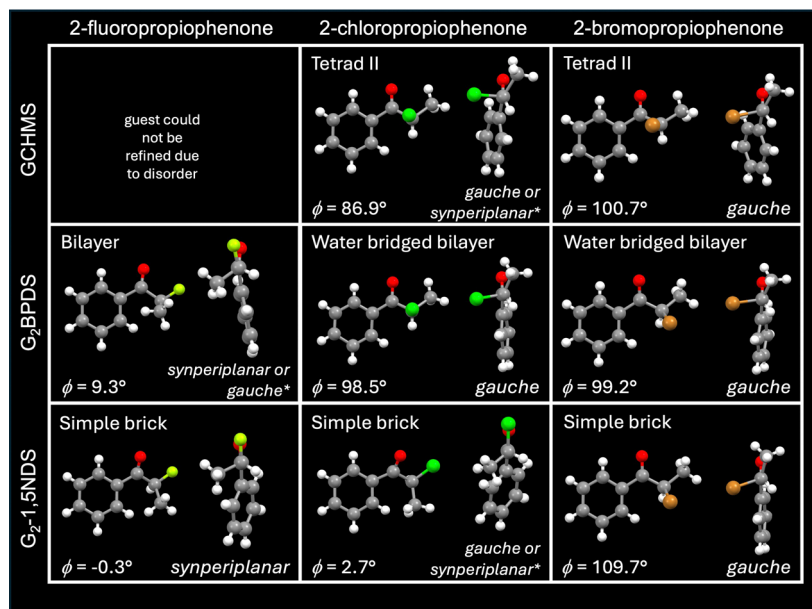


Fig. 4 Summary of the structural features for the host frameworks (rows) and their **F**, **Cl**, and **Br** guest molecules (columns). Each guest is portrayed in two orientations: (left) perpendicular to the plane of the phenyl ring, (right) along the C–C bond of the O–C–C–X dihedral angle. *The positions of the halogen and methyl group in these cases is ambiguous (see text), such that two conformations are possible in unspecified ratios. The anticalinal conformation can be ruled out in all cases, however.

with widths that increase in the order $\text{G}_2\text{1,5NDS} \supset \text{F}$ (7.483 Å) $<$ $\text{G}_2\text{1,5NDS} \supset \text{Cl}$ (7.659 Å) $<$ $\text{G}_2\text{1,5NDS} \supset \text{Br}$ (7.760 Å). The channel widths of the first two in the series fall within the typical range of 7.5 ± 0.2 Å for GS hosts (a_1 , Fig. 1). The void volume (with guests removed) increases in the same order, reflecting the compliance of the host framework that accommodates the steric requirements of the different guests. The larger channel width and void volume for $\text{G}_2\text{1,5NDS} \supset \text{Br}$ can be attributed to the perturbed GS sheet, wherein a subtle change in the alignment of adjacent ribbons is accompanied by a loss of one hydrogen bond (Fig. S3, ESI†). This observation illustrates that the GS sheet can sustain a decrease in hydrogen bonding to accommodate the larger guest while permitting its inclusion as its preferred *gauche* conformer, which accounts for about 80% of the population in methanol.⁸

Computations indicate that **Cl** prefers the *gauche* conformer (*ca.* 70 : 30 *gauche* : *synperiplanar* in methanol).⁸ The assignment of these two conformers in $\text{G}_2\text{1,5NDS} \supset \text{Cl}$ and $\text{GCHMS} \supset \text{Cl}$, proved ambiguous owing to positional disorder of the guest and low occupancy of the halogen, which clouded the location of these chloro and methyl substituents. It is likely that some distribution of the *synperiplanar* and *gauche* conformations may exist within the framework, reflecting the presence of both in methanol as expected from computations.

The observed conformers in the GS frameworks are consistent with the stabilization energies calculated for the *gauche* conformation ($\sigma_{\text{C}-\text{X}} \rightarrow \pi_{\text{C}-\text{O}}^*$), which increase in the order **F** $<$ **Cl** $<$ **Br**, whereas the *synperiplanar* conformation ($\sigma_{\text{C}-\text{Me}} \rightarrow \pi_{\text{C}-\text{O}}^*$) decreases in the order **F** $>$ **Cl** $>$ **Br**.⁸ **F** gains more hyperconjugative stabilization through $\sigma_{\text{C}-\text{Me}} \rightarrow \pi_{\text{C}-\text{O}}^*$ in the *synperiplanar* conformation than it would for $\sigma_{\text{C}-\text{X}} \rightarrow \pi_{\text{C}-\text{O}}^*$ in the *gauche* conformation

($\Delta = 3.13$ kcal mol⁻¹), while the opposite is true in the case of **Br** ($\Delta = -2.43$ kcal mol⁻¹). Meanwhile, the difference in stabilization energy between $\sigma_{\text{C}-\text{Me}} \rightarrow \pi_{\text{C}-\text{O}}^*$ and $\sigma_{\text{C}-\text{X}} \rightarrow \pi_{\text{C}-\text{O}}^*$ for **Cl** is minor ($\Delta = -0.34$ kcal mol⁻¹).

The observed conformational preferences of the encapsulated α -halopropiophenones reflect statistical distributions of the O–C–C–X dihedral angles in crystal structures reported for acyclic α -halo-substituted ketones found in the Cambridge structural database (CSD).⁹ Surveys of the CSD were performed for four fragments intended to mimic the α -halogenated ketones (Fig. 5). The conformational preferences observed in the GS inclusion compounds of **F**, **Cl**, and **Br** agree with the trends observed for crystal structures of analogous crystalline α -halo ketones in the CSD (details are provided as ESI†).

α -Halocyclooctanones. 2-Chlorocyclooctanone and 2-bromocyclooctanone (Fig. 1C), which exist as liquids at room temperature, were encapsulated in the GCHMS host. Analysis of the crystal structure of the guest revealed one conformer in $(\text{GCHMS})_3 \supset$ 2-bromocyclooctanone, classified as *gauche* (resembling the chloro-analogue in Fig. 5A), with $\phi_{\text{O}-\text{C}-\text{C}-\text{Br}} = 99.4^\circ$. In contrast, two conformers of 2-chlorocyclooctanone were observed in the $(\text{GCHMS})_3 \supset$ 2-chlorocyclooctanone inclusion compound. These conformers

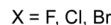
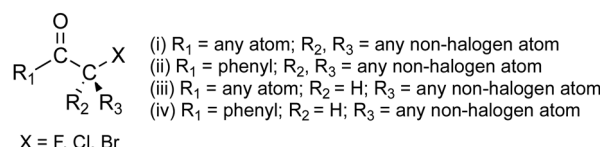


Fig. 5 Four fragments used for the Cambridge Structural Database (CSD) surveys (i)–(iv) of acyclic α -halo-substituted ketones.

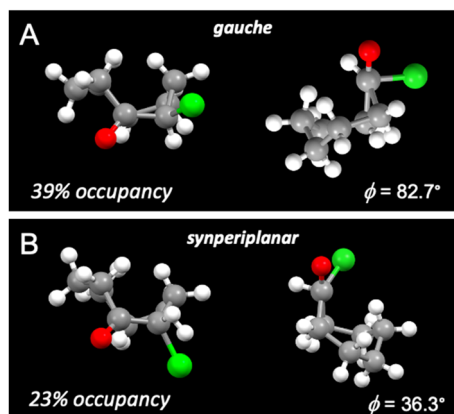


Fig. 6 The crystal structure of 2-chlorocyclooctanone guest encapsulated in GCHMS reveals two conformers (A) *gauche* (39% occupancy), and (B) *synperiplanar* (23% occupancy), and their respective O–C–C–Cl dihedral angles (ϕ). The remainder of the guests were disordered and could not be refined. The structures on the right correspond to their respective Newman projections.

resemble the *gauche* and *synperiplanar* conformations (Fig. 6), with occupancies of 39% and 23%, respectively (the remaining 38% of the electron density was too disordered to refine).

The conformations of 2-chlorocyclooctanone and 2-bromo-cyclooctanone observed in the GCHMS host were consistent with the computed lowest energy conformers. Calculations revealed that chair-boat conformations were lowest in energy, and the lowest energy conformer is described by a *gauche* conformation wherein the halogen atom is oriented equatorially on the boat side of the carbonyl group.¹⁰ The next lowest energy conformer is described by a *synperiplanar* conformation wherein the halogen atom is oriented axially on the boat side of the carbonyl group (Fig. S5, ESI†).¹⁰ These calculations revealed that the energy difference between these two conformers, for both compounds, decreased with increasing solvent polarity. The observation of both *gauche* and *synperiplanar* conformers of 2-chlorocyclooctanone in the GCHMS framework aligns with the small energy differences (*ca.* 0.5 kcal mol^{−1} calculated in CH₃CN) and the sensitivity of their energy ranking to the computational method used.¹⁰ For example, the energy difference calculated at the B3LYP level corresponds to $K_{\text{eq}} = 0.47$ (at 273 K) for the equilibrium *gauche* \rightleftharpoons *synperiplanar*, compared with $K_{\text{eq}} = 0.59$ (at 100 K) obtained from the crystal structure, demonstrating reasonable agreement between the occupancy distribution and computations.

This investigation has revealed that the preferred conformers of α -halopropiophenones were confirmed in most of the inclusion compounds here. Conformational assignment in three examples was ambiguous, although consistent with the two most preferred conformations. Furthermore, two α -halocyclooctanones were included in the adaptable GCHMS host, and the lowest energy conformer was observed for 2-bromocyclooctanone. In contrast, multiple conformers of 2-chlorocyclooctanone were observed, consistent with the small energy differences between the conformers. These results demonstrate that, in most cases, the GS hosts

allowed the guests to adopt their lowest-energy conformation. The ambiguity in the aforementioned three examples can be attributed to positional disorder of the guest owing to a “loose fit” of the guest in the host cavities, which prevented localization of the halogen atoms. These findings suggest that the use of GS frameworks for elucidating conformations of guests is promising, with implications for understanding stereochemical outcomes of their reactions.⁶ The results, however, reveal the importance of judicious selection of “Goldilocks” host frameworks that allow the guest to adopt its lowest energy conformation without undue influence by packing forces exerted by the host, while immobilizing the guest sufficiently to reduce positional disorder.

This work was supported by the National Science Foundation GOALI program through Award No. DMR-2002964. K. A. W. thanks the National Institute of General Medical Sciences of the National Institute of Health under Award No. 1R35GM148203-01. A. M. D. was supported partially by the Margaret Strauss Kramer Fellowship. The authors thank Dr Chunhua (Tony) Hu, Dr Mohammad Chaudhry, Dr Justin Newman, Dr Lee Daniels at Rigaku and Dr Michelle Neary at Hunter College (with support from the Air Force Office of Scientific Research under Award FA9550-20-1-0158) for collecting diffraction data for some compounds.

Data availability

CCDC numbers 2123655, 2307222, 2307223, and 2364251–2364258. Experimental methods, crystal data and crystallographic information files, supporting figures and CCDC conformation survey results.

Conflicts of interest

There are no conflicts to declare.

Notes and references

- 1 A. Yusov, A. M. Dillon and M. D. Ward, *Mol. Syst. Des. Eng.*, 2021, **6**, 756–778.
- 2 T. Adachi and M. D. Ward, *Acc. Chem. Res.*, 2016, **49**, 2669–2679.
- 3 K. T. Holman, A. M. Pivovar, J. A. Swift and M. D. Ward, *Acc. Chem. Res.*, 2001, **34**, 107–118.
- 4 A. Yusov, A. M. Dillon, M. T. Chaudry, J. A. Newman, A. Y. Lee and M. D. Ward, *ACS Mater. Lett.*, 2023, 1906–1912.
- 5 Y. Li, S. Tang, A. Yusov, J. Rose, A. N. Borrfors, C. T. Hu and M. D. Ward, *Nat. Commun.*, 2019, **10**, 4477.
- 6 N. D. Bartolo, K. M. Demkiw, J. A. Read, E. M. Valentín, Y. Yang, A. M. Dillon, C. T. Hu, M. D. Ward and K. A. Woerpel, *J. Org. Chem.*, 2022, **87**, 3042–3065.
- 7 A. M. Dillon, A. Yusov, M. T. Chaudry, J. A. Newman, K. M. Demkiw, K. A. Woerpel, A. Y. Lee and M. D. Ward, *Cryst. Growth Des.*, 2024, **24**, 3483–3490.
- 8 C. B. Francisco, C. D. S. Fernandes, F. Franco Dourado, G. D. F. Gauze, R. Rittner, R. S. Prosser and E. A. Basso, *J. Phys. Chem. A*, 2024, **128**, 1566–1575.
- 9 C. R. Groom, I. J. Bruno, M. P. Lightfoot and S. C. Ward, *Acta Crystallogr.*, 2016, **72**, 171–179.
- 10 T. C. Rozada, G. F. Gauze, F. A. Rosa, D. C. Favaro, R. Rittner, R. M. Pontes and E. A. Basso, *Spectrochim. Acta, Part A*, 2015, **137**, 176–184.